ADVANCED ENERGY MATERIALS
www.advenergymat.de

Nonpolar Alkanes Modify Lithium-Ion Solvation for Improved Lithium Deposition and Stripping

Chibueze V. Amanchukwu, Xian Kong, Jian Qin, Yi Cui, and Zhenan Bao**

Lithium metal batteries have been plagued by the high reactivity of lithium. Reactive additives that can passivate the lithium metal surface and limit electrolyte accessibility to a fresh lithium surface have been widely explored, but can have limited utility with continuous consumption of the additive. In this work, an alternative strategy is explored. The use of nonreactive cosolvents such as nonpolar alkanes is studied and its is shown that hexane and cyclohexane addition to ether solvents (1,3-dioxolane and 1,2-dimethoxyethane) halves the nucleation and growth overpotentials for lithium deposition, increases the cell coulombic efficiency, improves the lithium deposition morphology, increases the electrolyte oxidative stability (>0.2 V), and doubles the cycle life—even when compared to a widely used fluorinated ether. The nonpolar alkanes modify the lithium-ion solvation environment and reduce the solvation free energy; hence reducing the reaction barrier for lithium deposition. Exploration of nonpolar alkanes as part of the electrolyte mixture is a promising strategy for controlling metal deposition.

1. Introduction

The development of rechargeable energy storage media with high capacities is needed for the electrification of transport and stabilization of a renewable energy-dominated grid. Current lithium-ion batteries have the highest energy densities commercially available, but batteries with even higher energy densities are needed for electric vehicle use and for the electric grid.[1–6] One pathway of great interest is the replacement of the current graphitic anode in lithium-ion batteries with lithium metal.[5,6] Lithium metal has an order of magnitude higher specific capacity (3860 mAh g^{-1}), a lower reduction potential (–3.04 V), and can be paired with numerous cathode chemistries to yield batteries with higher energy densities.[5,6] However, lithium metal has been studied for over five decades and many challenges persist.[5–7] Lithium metal is highly reactive—a consequence of its low reduction potential—and continuous reactivity with the electrolyte leads to electrolyte loss and severe capacity fade.[5,6]

Several approaches have been pursued to limit the side reactions that lithium may undergo with the electrolyte.[5,7] First, carbonate solvents primarily used in Li-ion batteries have been eschewed for ethers (1,3-dioxolane (DOL) and 1,2-dimethoxyethane (DME)) that show much higher Coulombic efficiencies upon lithium deposition and stripping.[7,8] Second, strategies such as the use of high salt content with the so-called "solvent-in-salt" systems have shown promise despite the high cost and high viscosity of the electrolyte solutions.[9–12] Furthermore, polymer coatings have been shown to support smooth lithium deposition.[13,14] Despite all—and in combination with—these strategies, the use of additives is paramount.[7] Additives are chosen that can preferentially react with lithium metal and passivate the surface, thereby limiting further reaction with the electrolyte and extending cycle life.[5,7,15] A plethora of additives such as inorganic salts (e.g., $LiNO_3$),[8,16] phosphates,[17] water,[18] solvents,[19] and fluorinated compounds,[20,21] among others have been explored.[7] Their working principle is as follows: these additives react with lithium metal to create a modified solid electrolyte interface (SEI) that is better able to stabilize the lithium metal surface. However, these additives continually react with any fresh lithium metal surface that is generated during cycling. Upon complete consumption of the additive, little is known about the lithium metal behavior. A recent study by Gasteiger et al.[22] provides important insight. They show that the cell Coulombic efficiency drops by over 60% upon consumption of the electrolyte additive (the widely used fluoroethylene carbonate) in Si-C composite anodes (which upon lithiation also reacts with and consumes the electrolyte like lithium metal). Increasing the additive concentration is often not a solution because of cost, decreased ionic conductivities, and possible hindrance of the desired redox kinetics. Hence, reactive additives may have limited utility because their continuous consumption will lead to a regime where the additive is no longer present and there is significant degradation in performance. Therefore, it is important to explore an alternative strategy: the development of nonreactive additives.[23,24] These nonreactive

Dr. C. V. Amanchukwu, Dr. X. Kong, Prof. J. Qin, Prof. Z. Bao
Department of Chemical Engineering
Stanford University
Stanford, CA 94305, USA
E-mail: zbao@stanford.edu
Prof. Y. Cui
Department of Materials Science and Engineering
Stanford University
Stanford, CA 94305, USA
E-mail: yicui@stanford.edu
Prof. Y. Cui
Stanford Institute for Materials and Energy Sciences
SLAC National Accelerator Laboratory
Menlo Park, CA 94025, USA

DOI: 10.1002/aenm.201902116

additives or cosolvents—if carefully designed—can reduce the surface concentration of electrolyte solvent at the lithium metal/electrolyte interface,[25] while remaining permanently present in the cell.

The high reactivity of lithium metal has made the pursuit of nonreactive additives challenging. However, there are a plethora of compounds that are stable against lithium metal. For example, highly reactive alkali metals (lithium and sodium) and strong Lewis bases (butyllithium and sodium hydride) are typically stored in mineral oil or paraffin oil.[26] Mineral oil—a long chain alkane—has no polar functional groups that may make it susceptible to undesired redox reactions with lithium metal. However, the lack of polar functional groups means that alkanes do not dissociate lithium salts. Inspired by this, we show that the addition of small molecule alkanes in lithium salt-containing ether solvents changes the lithium-ion solvation structure in the electrolytes, decreases the solvation free energy, and the nucleation and growth overpotentials required for lithium deposition and stripping. We observed much improved Li/Li cycling performance that correlates with higher alkane content, an improved lithium deposition morphology, and an increase in the oxidative stability of the electrolyte mixture. At the salt concentrations studied, these alkane systems also outperform a widely studied reactive fluorinated additive—TTE (1,1,2,2-tetrafluoroethyl 2,2,3,3-tetrafluoropropylether).[27,28] This work introduces a new concept of the use of nonreactive and nonpolar alkane cosolvents in the electrolyte that can greatly improve battery performance, and we show that controlling ionic solvation is vital; providing an additional knob to control metal deposition and stripping. Furthermore, the large number of alkanes available (and their low cost) makes the potential wide-ranging for a variety of battery chemistries, and could enable the development of high energy density batteries that are required for the electric revolution in transport and a renewable-dominated grid.

2. Results and Discussion

2.1. Rationale for Molecule Selection and Study

Lithium metal is stable in the presence of linear alkane media such as mineral oil.[26] Mineral oil is highly viscous; hence we focused on shorter chain alkanes such as *n*-hexane with a similar chemical structure to mineral oil, but with low molecular weight and viscosity. Because hexane is nonpolar (and cannot solvate lithium salts), we need a polar solvent that is miscible with hexane, but can also dissolve lithium salts. DOL and DME were chosen for this work because they have been heavily explored for lithium metal deposition and stripping, and have been shown to yield higher Coulombic efficiencies than carbonate-based solvents used in Li-ion batteries.[7,29] For the salt, we chose the commonly used lithium bis(trifluoromethane) sulfonimide (LiTFSI) with its highly delocalized anion.[7] A salt concentration of 0.1 M was used widely in this study because it allows us to probe the true influence of the solvent and additive. At high salt concentrations, it is known that the SEI is dominated by anion decomposition,[10,11] and it becomes difficult to probe how the solvent and additive affect properties such as nucleation and growth, and to decouple the salt versus additive effect. Fluorinated solvent additive—TTE—was chosen to serve as the comparison to the hexane system because TTE has been heavily explored for lithium metal use.[28,30] Unlike hexane, TTE is expected to react with lithium metal,[31] and should give insight into reactive versus nonreactive additives and their effect on lithium deposition and stripping. The molecular structures of these compounds are shown in **Figure 1**a, and relevant properties are listed in Table S1 in the Supporting Information.

2.2. Electrical Properties

The electrical properties of these novel electrolyte mixtures were explored. The 0.1 M LiTFSI concentration in a 1:1 volume ratio of DOL:hexane is completely miscible. Electrochemical impedance spectroscopy (EIS) was performed to observe the influence of these molecular changes on ionic transport. Figure 1b shows Nyquist plots for three different electrolyte mixtures at 30 and 0 °C. As Figure 1c and Figure S1 in the Supporting Information show, the solution resistance for the DOL and DOL:hexane mixtures is similar, with the DOL:hexane solution resistance slightly lower and yielding higher ionic conductivity (Table S2, Supporting Information). This is remarkable because despite a reduction of the volume of polar DOL present by hexane addition, there is no significant reduction in ionic conductivity, and the electrolyte resistance remains roughly constant as a function of temperature (Figure 1c). We ascribe this improvement in conductivity to a reduction in solution viscosity with hexane addition (Table S3, Supporting Information) and higher lithium diffusivity (discussed later). In contrast, when TTE is added, the solution resistance increases (Figure 1b), and an Arrhenius-like relationship is observed for the resistance dependence on temperature (Figure 1c).

2.3. Influence on Electrochemistry

The influence of the electrolyte mixtures on lithium deposition and stripping was studied. Lithium/lithium symmetrical cells were fabricated, and before any electrochemistry was performed, the cell impedance was recorded. Figure S2 in the Supporting Information shows that the interfacial (and solution) resistance is lowest for DOL:hexane mixtures and highest for DOL:TTE mixtures, mirroring the conductivity measurements in Figure 1. Hexane addition appears to lead to an improved lithium/electrolyte interface that will bode well for lithium electrochemistry. In contrast, the cell impedance for the TTE mixture is an order of magnitude higher, indicating a poor lithium–electrolyte interface.

Galvanostatic deposition of lithium was performed and **Figure 2**a shows the definition of nucleation and growth overpotentials as discussed in this work.[29] Figure 2b shows that the nucleation overpotential required to deposit lithium is lowest for the DOL:hexane mixture and highest for the TTE mixture. Furthermore, the time (or capacity) required for the nucleation event is lowest for the DOL:hexane mixture and highest for the DOL:TTE mixture. The nucleation behavior observed in Figure 2b is reproducible across multiple cells, and at different

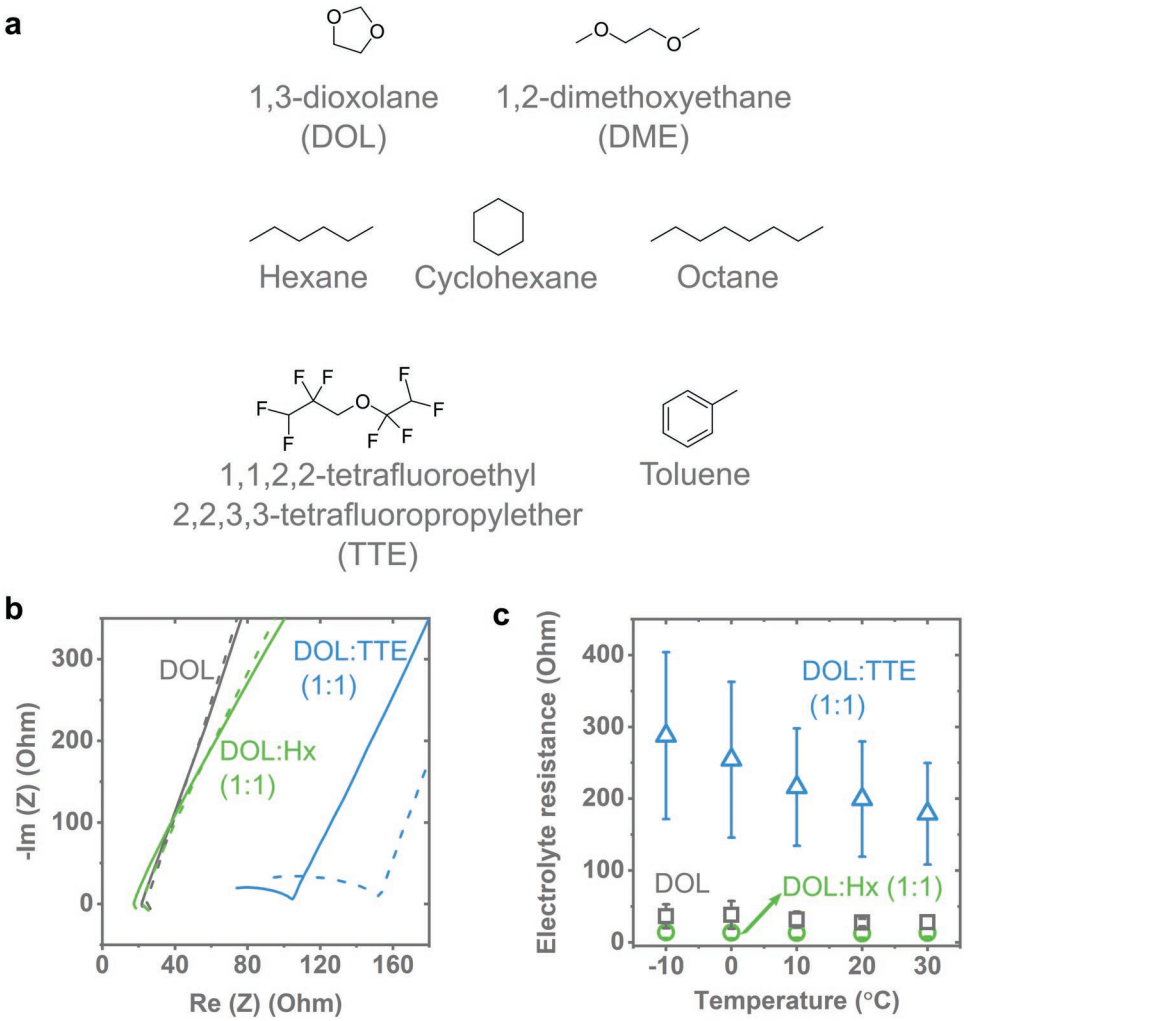

Figure 1. Chemical structures and electrical properties of the electrolytes. a) DOL and DME are polar solvents to dissolve salt. Nonpolar solvents (*n*-hexane, cyclohexane, *n*-octane) are added as the nonreactive additives and compared to TTE (reactive fluorinated additive) and toluene (nonpolar but aromatic). b) EIS Nyquist plots of the electrolyte mixtures at 30 °C (bold) and 0 °C (dashed) and c) total electrolyte resistance (contact + bulk resistance) as a function of temperature. The values in parenthesis (e.g., 1:1) refers to volume ratios. Salt concentration: 0.1 M LiTFSI. Hx: Hexane. Error bars in (c) represent the standard deviation at each temperature.

current rates (Figure S3, Supporting Information). Although the nonreactivity of hexane motivated its use in this work, the ability of the hexane mixture to reduce the nucleation overpotential is unexpected. It is known that impurities such as water can impact nucleation overpotentials. Hence, the electrolyte solvents were stored under activated 4 Å molecular sieves, and a new batch of electrolyte was made each time new battery cells were fabricated. Furthermore, commercial *n*-hexane with different purity levels (95% and 99.7% where the impurities are other hexane isomers) was also evaluated, and regardless of the hexane purity level, the observations are consistent (Figure S4, Supporting Information).

More importantly, the growth overpotential for continued lithium deposition and stripping is lowest in the hexane mixture (Figure 2c) and is a function of hexane content (Figure 2d). As the cosolvent amount is increased with hexane addition, the nucleation overpotential is decreased compared to the DOL and DOL:TTE mixture. While the initial nucleation overpotential does not appear to linearly decrease with hexane mole fraction in the electrolyte, the 3rd deposition overpotential does linearly decrease with hexane mole fraction. When cycled at 0.5 mA cm^{-2} to 0.5 mAh cm^{-2}, Figure 2e shows the inability of the 0.1 M LiTFSI in DOL:TTE (1:1 v/v) to support long-term lithium deposition and stripping. While this observation may seem to contradict previous work done with TTE,[31] Figure S5 in the Supporting Information shows that a higher salt concentration of 1 M (similar to previously published work) leads to improved performance compared to 0.1 M DOL:TTE. Remarkably, the 1 M LiTFSI in DOL:TTE (1:1 v/v) matches the 0.1 M LiTFSI in DOL:hexane (1:1 v/v) mixture despite the order of magnitude disparity in salt content and the presence of TTE; illustrating the unique impact of using nonpolar alkanes (Figure S5, Supporting Information). Maximizing the salt content in the DOL:hexane (1:1 v/v) mixture to 0.2 M LiTFSI can also improve the cycling behavior (Figure S6, Supporting Information). Utilization of hexane-soluble lithium salts[32,33] or

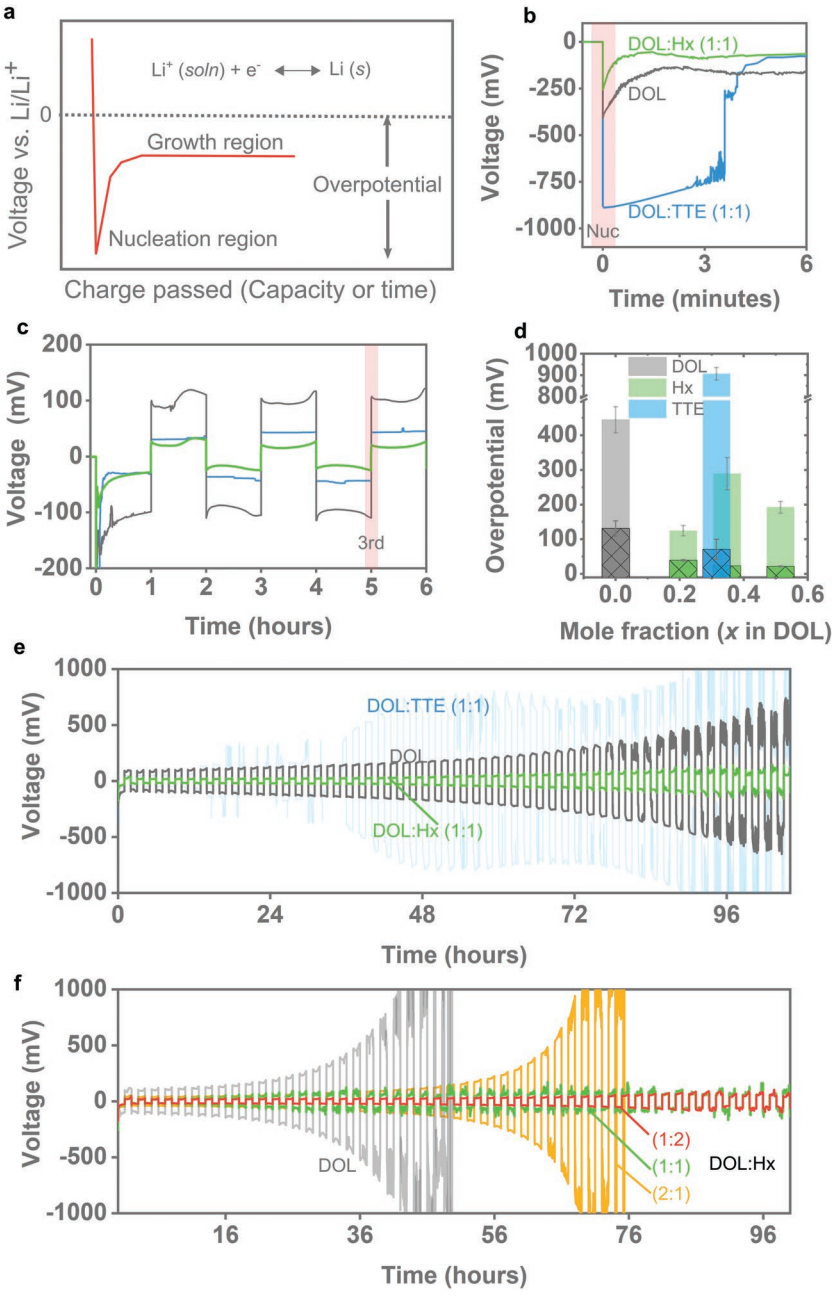

Figure 2. Lithium deposition and stripping in lithium symmetric cells with different electrolyte mixtures. a) Schematic illustrating the definition of nucleation and growth overpotentials. b) Nucleation overpotentials associated with lithium deposition in Li/Li cells using different electrolyte mixtures at a current density of 1 mA cm^{-2}. c) Subsequent deposition and stripping potentials at a current density of 1 mA cm^{-2} to a capacity of 1 mAh cm^{-2} for the different electrolytes. d) Nucleation and growth overpotentials for different electrolyte mixtures where the lightly shaded region refers to the nucleation region highlighted in (b) and the dark crossed region refers to the 3rd deposition overpotential highlighted in (c). Long-term Li/Li cycling at e) 0.5 mA cm^{-2} to 0.5 mAh cm^{-2} and f) 1 mA cm^{-2} to 1 mAh cm^{-2} where the ratios in (e) represents different DOL:hexane volume ratios. The ratios in parenthesis (e.g., 1:1) are volume ratios. All concentrations are 0.1 M LiTFSI in the varying solvent mixtures.

the addition of surfactants to prevent phase separation in the mixtures could be further explored to increase salt solubility. Again, as mentioned previously, this work purposefully utilizes low salt concentration to understand the effect of the solvent and additive, without masking their effect due to dominant salt anion decomposition. While the 0.1 M LiTFSI in DOL can cycle, increasing the current rate from 0.5 mA cm^{-2} (Figure 2e) to 1 mA cm^{-2} (Figure 2f) leads to a faster rise in overpotentials and cell death. Figure 2f shows that as the volume ratio of hexane increases, the following occurs: decrease in the nucleation and growth overpotentials and improved cycle life. Remarkably, moving to a 0.1 M LiTFSI in DOL:hexane (1:2) ratio leads to even better long-term cycling, even though the 1:2 ratio is not completely miscible. However, the trends of significant improvement with hexane addition is clear. Finally, we fabricated Li/$LiFePO_4$ (LFP) cells using the hexane electrolyte, and Figure S7 in the Supporting Information shows that the hexane mixture can support Li/LFP cycling.

2.4. Electrochemistry in Lithium/Copper Cells

We fabricated lithium/copper cells with different electrolyte mixtures to further probe the deposition and stripping kinetics. Li/Cu cells allow for careful probing of the lithium electrochemistry, morphology, and interfacial composition. As expected, **Figure 3**a shows that the observed trends in Figure 2 are maintained. It is important to note that although we maintain the 0.1 M salt content in the DOL:hexane (1:1 v/v) mixture, the entire salt is dissolved in DOL; hence it could be considered a 0.2 M DOL solution (see Note S1, Supporting Information). To provide a complete picture, we also perform deposition and stripping with 0.2 M in DOL and 1 M in DOL cells. Again, the nucleation overpotential is lowest in the 0.1 M DOL:hexane (1:1 v/v) when compared to 0.1 M DOL and 0.2 M DOL. The improvement of the hexane mixture compared to the 0.2 M mixture shows that electrochemically a 0.1 M DOL:hexane mixture is not equivalent to 0.2 M DOL. Remarkably, despite the order of magnitude increase in salt content (and subsequent possible anion decomposition), the nucleation overpotential for the 1 M DOL is similar to the DOL:hexane mixture. Figure 3b shows that at longer times, the 0.1 and 0.2 M cells get progressively worse with higher overpotentials required for deposition. Meanwhile, the DOL:hexane mixture mirrors the 1 M DOL system. The difference in deposition overpotentials between 0.1 M DOL and DOL:hexane widens with further cycling, hinting at an increase in side reactions that

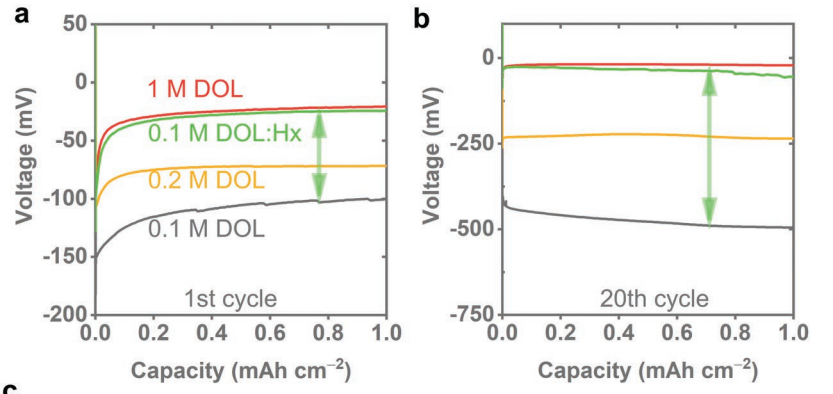

c

	0.1 M DOL	0.2 M DOL	0.1 M DOL:Hx (2:1)	0.1 M DOL:Hx (1:1)
Coulombic Efficiency (%)	89.6 ± 2	93.5 ± 1.2	97.4 ± 0.1	96.4 ±1

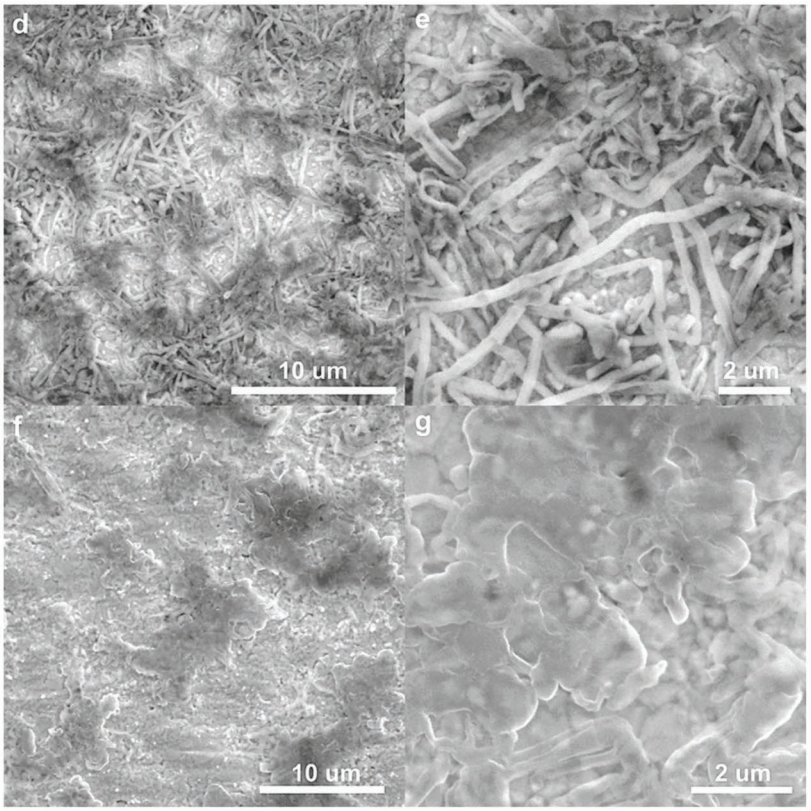

Figure 3. Effect of electrolyte mixtures on electrochemistry and morphology. Lithium deposition onto copper as a function of different salt concentrations in DOL compared to 0.1 M DOL:hexane (1:1 v/v) mixture at a) the initial deposition step and at b) the 20th deposition step. c) Coulombic efficiency values obtained using a modified Aurbach method[34,35] with Li/Cu cells. SEM images of lithium deposits on copper (1 mA cm^{-2} to 0.1 mAh cm^{-2}) using d,e) a 0.1 M DOL solution and f,g) a 0.1 M DOL:hexane (1:1 v/v) solution. Salt: LiTFSI. Hx: Hexane. The values in parenthesis in (c) are volume ratios. The reported Coulombic efficiencies are an average of at least three cells with standard deviation reported as the error.

exacerbate the amount of electrochemically-inactive lithium that is formed. The effect of hexane on the cell Coulombic efficiency was measured using Li/Cu cells with a modified Aurbach method (Figure S8, Supporting Information).[34,35] As Figure 3c shows, the addition of hexane in a 2:1 or a 1:1 v/v mixture increases the Coulombic efficiency from 89% in DOL to 97% with hexane addition, and also the charge/discharge efficiency across multiple cycles (Figure S9, Supporting Information). More importantly, the improvement cannot be completely ascribed to concentration effects, as the 0.2 M DOL electrolyte has lower Coulombic efficiency even when compared to both hexane mixtures. The Li/Cu data shown in Figure 3 are consistent with the Li/Li cells in Figure 2, and show the remarkable nature of the simple nonreactive nonpolar alkane to modify electrochemical behavior.

2.5. Morphological Study and Interfacial Composition

Scanning electron microscopy (SEM) was used to study the morphology of lithium deposited at different deposition capacities and cycles. We fabricated Li/Cu cells and deposited 0.1 mAh cm^{-2} of lithium to interrogate the initial deposition morphology. Figure 3d,e shows that when 0.1 M DOL is used as the electrolyte, clear dendrites are formed. These dendrites span the entire electrode. However, when a 0.1 M DOL:hexane electrolyte is used (Figure 3f,g), the density of dendrites present on the electrode surface is much lower. The lack of dominant dendrite formation may help explain the longer cycling lifetime observed in Figures 2 and 3a,b. The high surface area to volume ratio of dendrites can exacerbate reactions with the electrolyte and hasten cell death. At a growing lithium nuclei, the dynamic nature of the DOL:hexane mixture may present the nonconductive hexane solvent at the top of the growing nuclei, and prevent further growth because of the lack of lithium ions (effect on wetting discussed later). The dynamic nature of the electrolyte mixture may help smoothen deposition. We must note that just the addition of hexane does not prevent dendrite formation, but limits their proliferation across the entire electrode. At a higher deposition capacity of 1 mAh cm^{-2} (Figure S10, Supporting Information) and also after ten cycles (Figure S11, Supporting Information), it becomes difficult to distinguish the morphological difference. However, as the optical images in Figures S12 and S13 in the Supporting Information show, the SEI and "dead lithium" thickness after ten and 50 cycles are an order of magnitude higher without alkane addition. For example, after 50 cycles, both 0.1 and

0.2 M DOL Li/Cu systems have an "SEI + dead lithium" thickness of about 250 µm compared to 12 µm for the alkane mixture (Figure S13, Supporting Information).

X-ray photoelectron spectroscopy (XPS) was used to study the generated interfacial composition. Figure S14 in the Supporting Information shows XPS data after one deposition (1 mAh cm^{-2}), and there are no differences between the 0.1 M DOL and the DOL:hexane mixture. This is unsurprising because the components of both electrolytes are similar: LiTFSI and DOL, while the hexane is expected to be inert. The interface is dominated by LiTFSI decomposition products.[11] Even after ten cycles and with argon sputtering, the SEI composition appears similar between the DOL and DOL:hexane systems (Figure S15, Supporting Information). These XPS data suggest that the improvements in performance is not necessarily due to the SEI composition. This observation is quite different from what is typically observed in literature, where "fortifying" the SEI with inorganic LiF (using numerous reactive additives) correlates with improved deposition/stripping behavior.[36,37]

2.6. Expanding the Range of This Work

The concept of using nonreactive alkanes is quite powerful because it opens a multitude of compounds that can be studied. There are a significant number of alkanes and other nonpolar compounds that can be incorporated with polar solvents to improve electrochemical performance. The work has focused significantly on DOL and *n*-hexane. The question that remains: are the observations made with the DOL:hexane mixture applicable to other mixtures with nonreactive additives? The answer is yes.

The addition of cyclohexane to DOL also improves the electrochemical performance (**Figure 4**a and Figure S16, Supporting Information). Figure 4a shows Li/Li cells fabricated with a 0.1 M LiTFSI in DOL:cyclohexane (1:1 v/v) electrolyte where cyclohexane addition decreases the lithium nucleation and growth overpotential—similar to the DOL:hexane mixture—leading to better long-term cycling. The polar phase can also be changed from DOL to DME, and the same electrochemical trends are observed (Figure 4b and Figure S17, Supporting Information). Li/Li cells were fabricated with DME:hexane as the electrolyte medium. As *n*-hexane is added to DME, lower nucleation and growth overpotentials are observed (Figure 4b), and an increase in the hexane ratio further decreases the cycling overpotentials and improves cycle life; similar to DOL:hexane mixtures.

Furthermore, we perform electrochemical stability measurements of the electrolyte mixtures to understand the effect of the nonpolar additive and the accessibility of the polar solvent at the electrode surface. Using potentiostatic holds at increasingly higher voltages, Figure 4c shows that hexane addition to DME leads to an increase in the oxidation voltage of the electrolyte mixture (from 4.2 to 4.4 V). This observation lends credence to the hypothesis that hexane limits accessibility of the polar solvent to the working electrode, hence extending the voltage stability window before Faradaic reactions occur. We also explored the electrolyte oxidative stability against a $LiFePO_4$ electrode that is of commercial relevance. Figure S18 in the Supporting Information shows that against an LFP working electrode, alkane addition limits complete decomposition of the electrolyte at higher oxidation voltages. These results indicate that the nonpolar additive modifies the negative electrode (lower

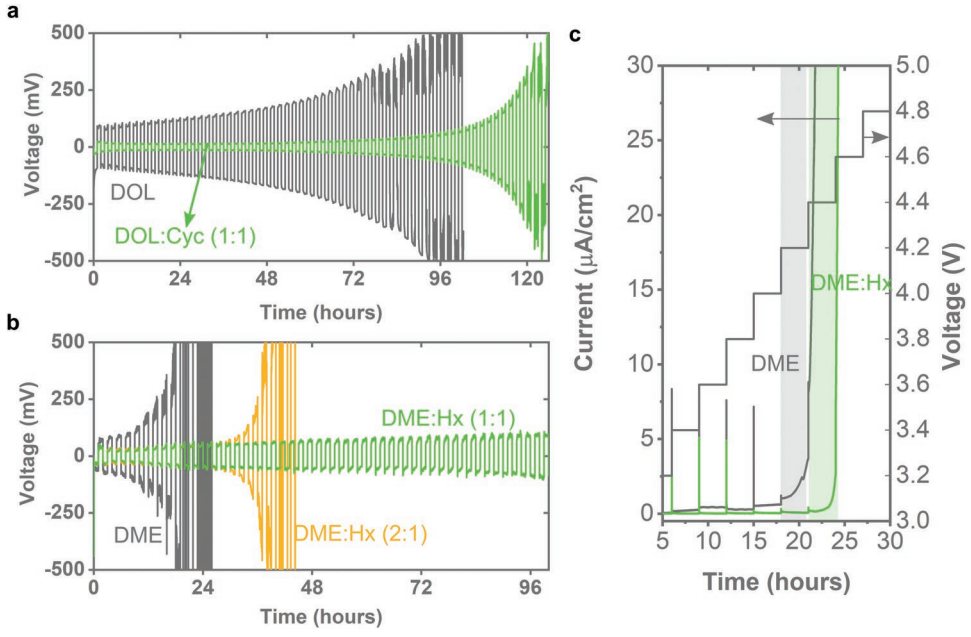

Figure 4. Lithium deposition and stripping in other polar:nonpolar mixtures. a) Lithium deposition and stripping profile in Li/Li cells with 0.1 M DOL and 0.1 M DOL:cyclohexane (1:1 v/v) electrolyte mixture at 0.5 mA cm^{-2} to 0.5 mAh cm^{-2}. b) Lithium deposition and stripping profiles in Li/Li cells with 0.1 M DME, 0.1 M DME:Hx (2:1 v/v) and 0.07 M DME:Hx (1:1 v/v) ratios at 1 mA cm^{-2} to 1 mAh cm^{-2}. c) Potentiostatic hold measurements in a two-electrode setup with a stainless steel (SS) working electrode where the SS is held at increasingly higher potentials for 3 h and the current response is measured for a 0.07 M DME and a 0.07 M DME:Hx (1:1 v/v) electrolyte mixtures. Salt: LiTFSI.

overpotential for lithium deposition) and the positive electrode (extended oxidative stability).

By changing the polar and nonpolar phase from DOL to DME and hexane to cyclohexane, we show the breadth of the observations made in this work, and their wide applicability to modify both the negative and positive electrodes.

2.7. Surface Coverage Effect

Our original hypothesis for exploring these nonreactive nonpolar solvents is that they can limit the accessibility of the polar solvent to the electrode surface; hence prolonging cycle life through a mechanism different from reactive additives that instead passivate the surface.[25] We term this the "surface coverage effect" (Figure S19, Supporting Information). Addition of hexane and cyclohexane (with lower surface tension) to polar solvents such as DOL and DME reduces the surface tension of the mixture[38] (Table S1, Supporting Information) and modifies the wetting behavior of the electrolyte on the electrode surface. Figure S19 in the Supporting Information shows that the DOL:hexane mixture wets a silicon substrate considerably better than DOL alone. To ensure our qualitative observation is not limited to only silicon substrates, Videos S1 and S2 in the Supporting Information show that the 0.1 M LiTFSI in DOL:hexane (1:1 v/v) undergoes a similar wetting behavior upon contact with lithium metal. The modification of wetting behavior shows that hexane is present at the lithium/electrolyte interface, and may help explain the improvement in long-term cycling (Figure 2), and the increase in oxidative stability observed in Figure 4c. However, the surface coverage effect hypothesis is not enough to explain the decrease in nucleation and growth overpotentials.

2.8. Solvation Effect

To better explain the decrease in nucleation and growth overpotentials, we probe the lithium-ion solvation environment in the different electrolyte mixtures. ^{1}H, ^{7}Li, and ^{19}F NMR spectroscopy were used to study the solvation changes. **Figure 5**a shows the ^{7}Li NMR spectra of a 0.1 M LiTFSI in DOL solution as the hexane volume content is increased. Despite maintaining the same salt concentration, the lithium peak shifts significantly downfield as a function of hexane content. Downfield shift (shift to higher frequencies) is observed due to deshielding of the electron cloud surrounding the nuclei of interest—a decrease in the electron cloud that opposes the externally applied magnetic field. Therefore, there is less ion pairing and a decrease in Lewis basicity around the lithium ion.[39,40] In these hexane mixtures, the lithium is poorly solvated and free to diffuse without a strong solvation shell.[40] The downfield shifts are also observed when a longer linear alkane (octane) or cyclic alkane (cyclohexane) is added to DOL (Figure 5a and Figure S20, Supporting Information).

In contrast, TTE binds to the Li^+ within the Li^+–DOL solvation shell and hence increases the electron density around the lithium ion, leading to an upfield shift in the ^{7}Li NMR spectrum (Figure 5a). The upfield shift is also observed when an aromatic molecule toluene—though nonpolar—is added to DOL. The electron cloud within toluene leads to cation–π interactions, an increase in electron density around the lithium ion and subsequently the upfield shift (compared to the downfield shift seen with alkane mixtures). Similar to the poor electrochemical behavior observed in the TTE mixture (Figure 2), the DOL:toluene electrochemical performance is also poor (Figure S21, Supporting Information). To clarify that the observations we have made is not due to salt concentration effects, we perform ^{7}Li on a 0.2 M DOL solution. It shows a similar peak as the 0.1 M DOL solution with a very slight upfield shift (Figure 5a). In typical high salt concentration electrolytes, increasing salt content leads to an upfield shift in the ^{7}Li peak, attributed to increased ion pairing and an increase in Lewis basicity around the lithium cation.[39] However, for the hexane mixtures, a downfield shift is observed, again illustrating the difference between these mixtures and high salt concentration systems. A schematic summarizing our current understanding on the effect of these electrolytes on lithium solvation is illustrated in Figure 5d.

The environment around the polar DOL solvent was also explored to help explain the ^{7}Li findings. Figure 5b shows ^{1}H data that complements the ^{7}Li data, and shows that both the Li^+ and DOL solvation environment are deshielded in the presence of nonpolar alkanes, but shielded upon addition of TTE or aromatic toluene. The effect of these electrolyte mixtures on lithium ion and TFSI anion diffusivity was measured using pulsed-field gradient (PFG) NMR.[41] Figure S22 in the Supporting Information shows that lithium ion diffusivity does not necessarily correlate with the upfield and downfield shifts observed in Figure 5, but with the viscosity of the added cosolvent to DOL (as expected through the Stokes–Einstein relation). However, the changes in ionic diffusivity and viscosity are minor, and do not appear to correlate with the ionic solvation structure and observed electrochemistry.

Classical molecular dynamics (MD) simulation was performed to probe the solvation environment around the lithium ion. Figures 5e–g shows radial distribution functions (RDFs) of different electrolyte mixtures next to a lithium ion. Across all systems, an increase in additive amount (hexane, cyclohexane, or TTE) leads to an increased probability of ether (DOL) presence around the lithium ion.[42] However, hexane and cyclohexane are not present within the first two solvation shells around lithium, but TTE is (dashed line in 5g). A snapshot of the first solvation shell at a distance (r = 0.33 nm) further confirms this and the inset in Figure 5g shows that TTE is present within the first solvation shell whereas the insets in Figure 5e,f do not show hexane or cyclohexane present.

The solvation free energy of a lithium ion solvated by different electrolyte mixtures was computed using classical MD. Figure 5c shows that upon hexane and cyclohexane addition to DOL, the magnitude of the lithium solvation free energy continually decreases. For TTE, the magnitude of the solvation free energy increases with higher TTE concentration. These MD simulations corroborate the NMR results in that they show looser Li^+ coordination and solvation with hexane or cyclohexane addition, and stronger Li^+ solvation with TTE addition. The ionic solvation behavior strongly correlates with the electrochemistry. Lithium-ion desolvation—the ability of

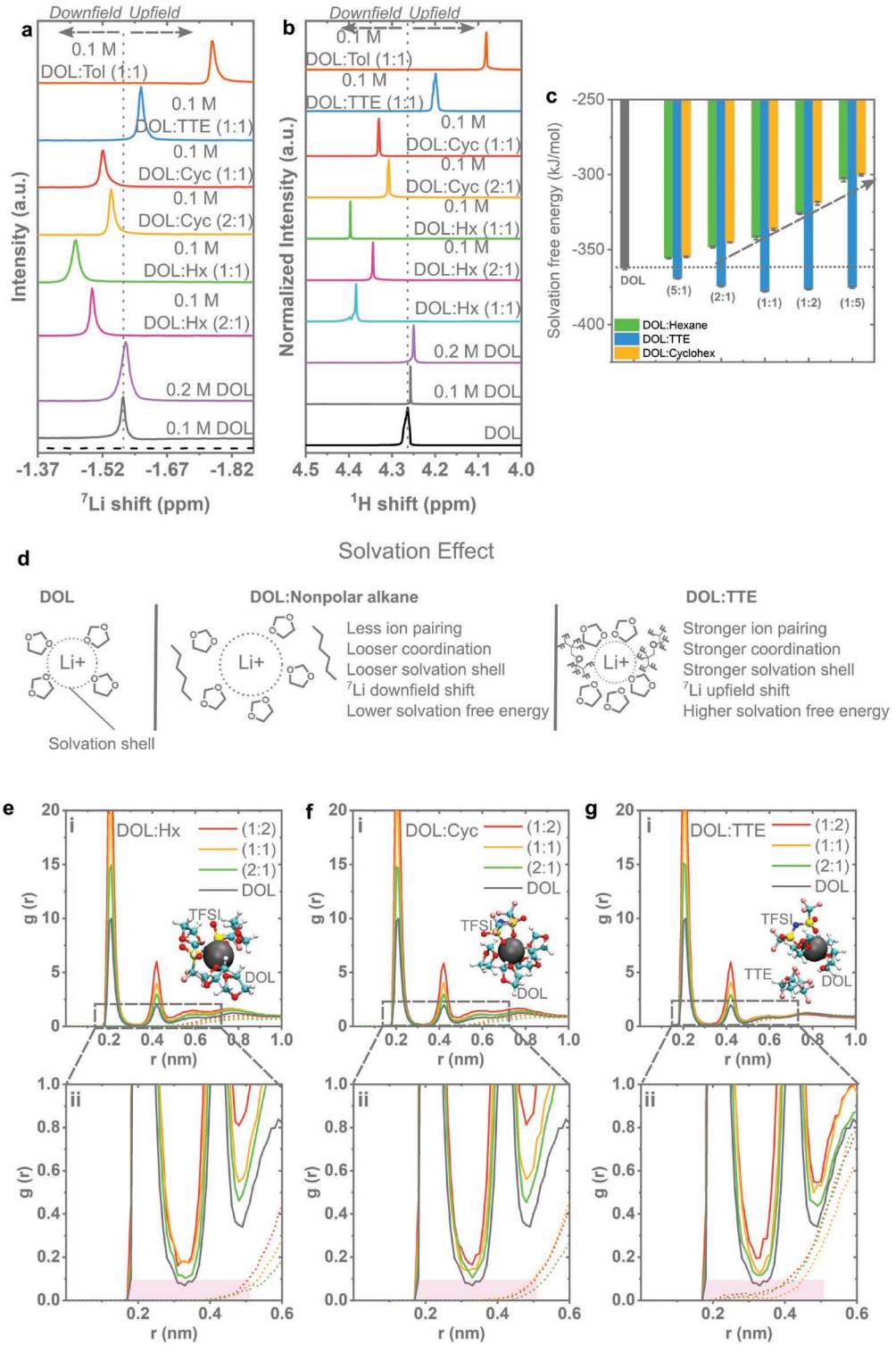

Figure 5. Solvation effect. a) ^{7}Li and b) ^{1}H NMR spectra of the different electrolyte mixtures. NMR was obtained using a capillary setup with the ^{7}Li NMR values referenced to 1 M $LiClO_4$ (–2.80 ppm)[46] in CD_3CN and ^{1}H NMR referenced to residual protons in CD_3CN (1.94 ppm). c) Computed lithium-ion solvation free energies in different electrolyte mixtures. d) Schematic illustrating the "solvation effect," and the impact on lithium solvation between DOL, DOL:nonpolar alkane (hexane or cyclohexane), and DOL:TTE electrolytes. RDFs of Li–O (bold) and Li–C (dashed) for a lithium ion in e) DOL:hexane mixture and f) DOL:cyclohexane mixture and g) Li–O (bold) and Li–F (dashed) for a lithium ion in DOL:TTE. The graphs in (ii) is a zoomed-in portion of the data in (i) for better visualization. The highlighted region in pink shows the differences between the alkanes and TTE, specifically the encroachment of TTE within the lithium solvation shell. Insets in (i) are snapshots of the solvation shell around lithium within 0.33 nm in a DOL:cosolvent (1:2 v/v) mixture (gray = lithium). The values in parenthesis (e.g., 1:1) in all the images refers to volume ratios. 0.1 M refers to the salt (LiTFSI) concentration in the respective electrolytes.

lithium to shed its solvation shell—in lithium-ion batteries has been implicated as a rate-limiting step in the charging of lithium batteries.[43,44] As Li^+ is poorly solvated in the hexane or cyclohexane mixture, the solvation free energy reduces and the overpotential required for deposition decreases—the chemical potential of the lithium ion is increased, and therefore the reaction energy barrier is lowered. The opposite trend is observed with TTE. TTE has often found use in electrolyte systems as a "nonsolvent" because it does not dissolve salt.[28,45] However, our NMR and computational work shows that nonsolvent TTE—despite a lack of salt solubility—can participate in lithium-ion solvation. Hence, the solvation free energy and "solvation effect" (Figure 5d) plays a significant role in explaining the effects of nonpolar alkane addition on lithium electrochemistry.

3. Conclusions

A new paradigm of nonreactive additives for the improvement of lithium metal systems has been proposed. We show that the addition of nonpolar solvents such as hexane and cyclohexane to ether solvents such as DOL and DME leads to a significant improvement in nucleation and growth overpotentials during lithium deposition and stripping, increased cell Coulombic efficiency, improved lithium deposition morphology from dendrites to a mossy/clump-like lithium, reduced SEI thicknesses, and more importantly prolonged cycling lifetime. The addition of these nonpolar alkanes to the polar solvent changes the ionic solvation of the lithium, leading to lower solvation free energies and lower lithium deposition and stripping overpotentials. In contrast, a typically used fluorinated cosolvent—TTE—binds with lithium ions and increases the solvation free energy leading to higher deposition and stripping overpotentials. We termed this the "solvation effect." The addition of nonpolar alkanes modify the wetting behavior of the electrolyte on the electrode, and improves the oxidative stability of the polar solvent. The nonpolar alkane appears to limit the accessibility of the polar solvent to the electrode surface; an observation we termed the "surface coverage effect." This opens an avenue for the study of nonpolar compounds in energy storage and conversion systems. The combination of nonpolar additives—that reduce polar solvent decomposition at the interface—with reactive additives—that can produce a strong robust SEI—could lead to longer-lived lithium-based batteries.

Experimental Section

Materials: DOL (anhydrous, 99.8%, with 75 ppm BHT inhibitor), DME (anhydrous, 99.5%, inhibitor-free), *n*-hexane (anhydrous, 95%), *n*-hexane (analytical standard, ≥99.7% purity), octane, cyclohexane (anhydrous, 99.5%), and toluene (anhydrous, 99.8%) were obtained from Sigma Aldrich. TTE was obtained from Synquest Laboratories. All solvents were stored under activated 4 Å molecular sieves in an argon glovebox before use. Lithium bis(trifluoromethane)sulfonimide was obtained from Solvay and was dried at 120 °C for two nights in an argon glovebox. Deuterated acetonitrile (D3, 99.8%) was obtained from Cambridge Isotope Laboratories. Lithium metal (750 µm thickness) was purchased from Alfa Aesar. $LiFePO_4$ (170 mAh g^{-1} theoretical capacity, loading of 12 mg cm^{-2}) was obtained as a single sided electrode coated on aluminum foil from MTI.

Electrolyte Preparation: All electrolytes were prepared in an argon glovebox (H_2O < 0.1 ppm, O_2 < 10 ppm). All electrolytes were prepared just before the cells were made, especially the hexane-based electrolytes because of the volatility of hexane. Furthermore, preparation of fresh electrolyte every time limited the influence of water because the solvents were stored in molecular sieves until the electrolyte was made. A predetermined amount of salt was measured in the glovebox and then solvent was added. For the hexane mixtures, the polar solvent (DOL or DME) was first added to the vial containing salt to fully dissolve the salt before the nonpolar solvent (hexane or cyclohexane) was added.

Battery Fabrication: In an argon glovebox, 2032 type coin cells were fabricated. Each cell utilized 60 µL of electrolyte and a single piece of Celgard 2325 separator. The lithium foil was scratched to reveal a lustrous metallic surface before the cells were fabricated. 1 cm^2 pieces of lithium was used. 2 cm^2 pieces of copper was used. 1 cm^2 $LiFePO_4$ electrodes were used. An Arbin Instruments Battery Tester was used for the Li/Li and Li/Cu cells. Li/Li cells were rested at open circuit voltage (OCV) for 24 h before cycling. Li/Cu cells were rested for 24 h at OCV and were precycled at 0.02 mA cm^{-2} for ten cycles before cycling was done at the predetermined current rate. The cells for oxidative stability were allowed to rest for at least 5 h before potentiostatic holds. The potentiostatic holds were performed using a Biologic MPG-2 from 3 to 6 V with 0.2 V steps and the cell held at each voltage for 3 h. A stainless steel (SS) electrode (2 cm^2) or an LFP electrode (1 cm^2) was used for the potentiostatic hold experiments.

Coulombic efficiency measurements were performed using a modified version of the Aurbach method that includes one precycle before initial deposition.[34,35] Specifically, in this work, the Li/Cu cells were first precycled at 0.5 mA cm^{-2} for one cycle. Then, 5 mAh cm^{-2} of lithium was deposited. Subsequently, 1 mAh cm^{-2} was deposited and stripped for a total of ten cycles at a current rate of 0.5 mA cm^{-2}. Finally, the remaining deposited lithium was stripped until 1 V. Sample data are shown in the Supporting Information (Figure S8, Supporting Information).

Impedance Spectroscopy: Coin cells were fabricated using two SS blocking electrodes, 1 Celgard 2325 separator, and 40 µL of electrolyte. Frequency ranges of 1 MHz to 1 Hz was used across the range of temperatures. A 10 mV perturbation was used. A Biologic VSP3 was used for the impedance measurements. For the temperature sweeps, an ESPEC chamber was used. The temperature sweeps were measured in cooling mode, with the first temperature at 30 °C for at least 2 h before the temperature was reduced to 20 °C (again held for 2 h before measurement) and so on. The cell constant used for the calculations of ionic conductivity was 7.75.

NMR Characterization: All NMR samples were prepared inside an argon glovebox. An NMR capillary setup was used where the electrolyte mixture was placed inside a capillary tube and sealed with a Teflon cap from the surrounding deuterated solvent. A 1 M $LiClO_4$ in deuterated acetonitrile was used as the internal standard because both its ^7Li and ^1H shifts did not interfere with the compounds of interest. The samples of interest were placed inside the capillary tube (≈100 µL). ^7Li, ^1H, and ^{19}F NMR were performed using Varian Inova 300 MHz NMR and a Varian 400 MHz Instrument. The ^7Li data were referenced to the Li in $LiClO_4$ (−2.80 ppm)[46] and the ^1H was referenced to the residual H in CD_3CN (1.94 ppm) (Figure S20, Supporting Information).

PFG NMR was used to study ion diffusivity. For the diffusivity measurements, the external 1 M $LiClO_4$ in CD_3CN solvent was removed. The sealed capillary tube containing the sample of interest was placed in an empty NMR tube. All diffusion measurements were made with the Varian 400 MHz at a temperature of 20.7 °C (the temperature was not controlled to limit effects of convection).[47] A pulse sequence with convection compensation was used for the ^7Li diffusion measurements (program "Dbppste_cc"). For ^{19}F and ^1H diffusion measurements, no convection compensation was needed (program "pgste"). ^7Li (duration pulse (δ) = 0.00325 s, interval of gradient pulse (Δ) = 0.528 s); ^{19}F (δ = 0.002 s, Δ = 0.529 s); ^1H (δ = 0.001–0.002 s, Δ = 0.132 s). Gradient strengths (g) of up to 15 G cm^{-1} was used. The area underneath the NMR curves (instead of peak intensity) was used for the fitting. Diffusion

constants were obtained through a linear fit to the following equation (γ = gyromagnetic ratio)[48]

$$I/I_0 = \exp\left(-\gamma^2 g^2 \delta^2 D\left(\Delta - \frac{\delta}{3}\right)\right) \quad (1)$$

SEM Characterization: The coin cells were opened inside an argon glovebox. The electrodes were not stored inside the glovebox to avoid contamination. They were immediately prepared for SEM analysis. The copper foil containing either lithium deposits or SEI was rinsed with fresh DOL to remove excess salt. Then, the electrodes were sealed and moved for SEM characterization. The sample was transferred immediately into the SEM chamber with minimal air exposure. A FEI Sirion was used for all the SEM characterization. Working voltage was 5 or 10 kV.

XPS Characterization: The coin cells were opened inside an argon glovebox. The electrodes were not stored inside the glovebox to avoid contamination. They were immediately prepared for XPS analysis. The electrodes were washed with fresh DOL before being placed in a sealed XPS transfer vessel. This ensured that the samples were not exposed to air at any time during sample preparation, sample transfer, and sample XPS analysis. A PHI Versaprobe I was used for the XPS analysis.

MD Simulation: MD simulations were performed using Gromacs 2018.[49] Optimized potentials for liquid simulations all atom[50] force field was used to describe molecules/ions used in this work. A cutoff of 12 Å was used to calculate both LJ interactions and the real part of electrostatic interactions, and the particle-mesh Ewald method was used to evaluate the long-range electrostatic interactions with a grid spacing of 1.2 Å. The temperature was controlled at 300 K using the Nosé–Hoover thermostat with a relaxation time of 0.2 ps. The pressure was controlled at 1 bar using Parrinello–Rahman barostat with a relaxation time of 2.0 ps. For equilibrium MD simulations, TFSI anions were put in the box to make the system net charge neutral. All properties were calculated after 2 ns equilibration runs. For lithium solvation free energy calculations, a typical system consisted of one lithium ion solvated in solvents. Interaction between Li^+ and the solvent molecules was scaled by a rescaling parameter λ. The interaction was turned on successively by changing λ from 0 to 1.0 at small steps (0.0, 0.1, 0.2, 0.3, 0.4, 0.5, 0.55, 0.6, 0.65, 0.7, 0.75, 0.8, 0.82, 0.84, 0.86, 0.88, 0.9, 0.92, 0.94, 0.96, 0.97, 0.98, 0.99, 1.0). The solvation free energy were estimated using the Bennett's acceptance ratio method.[51]

Supporting Information

Supporting Information is available from the Wiley Online Library or from the author.

Acknowledgements

C.V.A. conceived the idea and performed all experiments. X.K. performed the simulations. C.V.A. wrote the manuscript and X.K., J.Q., Y.C., and Z.B. discussed and revised the manuscript. The authors acknowledge the support from the Assistant Secretary for Energy Efficiency and Renewable Energy, Office of Vehicle Technologies of the U.S. Department of Energy under the Battery Materials Research (BMR) program and Battery 500 Consortium. C.V.A. acknowledges support from the California Alliance Postdoctoral Fellowship and the TomKat Center Postdoctoral Fellowship in Sustainable Energy at Stanford. SEM and XPS were performed at the Stanford Nano Shared Facilities (SNSF), supported by the National Science Foundation under award ECCS-1542152. NMR was performed at the NMR Facility in the Stanford Department of Chemistry. The authors thank Stephen Lynch, Minah Lee, Allen Pei, Paul Rudnicki, Wesley Michaels, and Snehashis Choudhury for fruitful discussions.

Conflict of Interest

The authors declare no conflict of interest.

Keywords

electrolytes, Ion solvation, lithium metal batteries, nonpolar alkanes, nonreactive additives

Received: June 30, 2019
Revised: August 15, 2019
Published online:

[1] C. V. Amanchukwu, H.-H. Chang, M. Gauthier, S. Feng, T. P. Batcho, P. T. Hammond, *Chem. Mater.* **2016**, *28*, 7167.
[2] C. V. Amanchukwu, H.-H. Chang, P. T. Hammond, *J. Phys. Chem. C* **2017**, *121*, 17671.
[3] C. V. Amanchukwu, J. R. Harding, Y. Shao-Horn, P. T. Hammond, *Chem. Mater.* **2015**, *27*, 550.
[4] C. V. Amanchukwu, M. Gauthier, T. P. Batcho, C. Symister, Y. Shao-Horn, J. M. D'arcy, P. T. Hammond, *J. Phys. Chem. Lett.* **2016**, *7*, 3770.
[5] D. Lin, Y. Liu, Y. Cui, *Nat. Nanotechnol.* **2017**, *12*, 194.
[6] M. D. Tikekar, S. Choudhury, Z. Tu, L. A. Archer, *Nat. Energy* **2016**, *1*, 16114.
[7] K. Xu, *Chem. Rev.* **2004**, *104*, 4303.
[8] F. Ding, W. Xu, X. Chen, J. Zhang, M. H. Engelhard, Y. Zhang, B. R. Johnson, J. V. Crum, T. A. Blake, X. Liu, J.-G. Zhang, *J. Electrochem. Soc.* **2013**, *160*, A1894.
[9] L. Suo, Y.-S. Hu, H. Li, M. Armand, L. Chen, *Nat. Commun.* **2013**, *4*, 1481.
[10] L. Suo, O. Borodin, T. Gao, M. Olguin, J. Ho, X. Fan, C. Luo, C. Wang, K. Xu, *Science* **2015**, *350*, 938.
[11] S. Jiao, X. Ren, R. Cao, M. H. Engelhard, Y. Liu, D. Hu, D. Mei, J. Zheng, W. Zhao, Q. Li, N. Liu, B. D. Adams, C. Ma, J. Liu, J.-G. Zhang, W. Xu, *Nat. Energy* **2018**, *3*, 739.
[12] J. Qian, W. A. Henderson, W. Xu, P. Bhattacharya, M. Engelhard, O. Borodin, J.-G. Zhang, *Nat. Commun.* **2015**, *6*, 6362.
[13] J. Lopez, A. Pei, J. Y. Oh, G.-J. N. Wang, Y. Cui, Z. Bao, *J. Am. Chem. Soc.* **2018**, *18*, 19.
[14] G. Zheng, C. Wang, A. Pei, J. Lopez, F. Shi, Z. Chen, A. D. Sendek, H.-W. Lee, Z. Lu, H. Schneider, M. M. Safont-Sempere, S. Chu, Z. Bao, Y. Cui, *ACS Energy Lett.* **2016**, *1*, 1247.
[15] J. Zheng, M. H. Engelhard, D. Mei, S. Jiao, B. J. Polzin, J.-G. Zhang, W Xu, *Nat. Energy* **2017**, *2*, 17012.
[16] D. Aurbach, E. Pollak, R. Elazari, G. Salitra, C. S. Kelley, J. Affinito, *J. Electrochem. Soc.* **2009**, *156*, A694.
[17] S. Chen, J. Zheng, L. Yu, X. Ren, M. H. Engelhard, C. Niu, H. Lee, W. Xu, J. Xiao, J. Liu, J.-G. Zhang, *Joule* **2018**, *2*, 1548.
[18] J. Qian, W. Xu, P. Bhattacharya, M. Engelhard, W. A. Henderson, Y. Zhang, J.-G. Zhang, *Nano Energy* **2015**, *15*, 135.
[19] X. Li, J. Zheng, X. Ren, M. H. Engelhard, W. Zhao, Q. Li, J.-G. Zhang, W. Xu, *Adv. Energy Mater.* **2018**, *8*, 1703022.
[20] S. Chen, J. Zheng, D. Mei, K. S. Han, M. H. Engelhard, W. Zhao, W. Xu, J. Liu, J.-G. Zhang, *Adv. Mater.* **2018**, *30*, 1706102.
[21] D. Talian, S. Jeschke, S. Vizintin, A. Pirnat, K. Arčon, I. Aquilanti, G. Johansson, P. Dominko, *Chem. Mater.* **2017**, *29*, 10037.
[22] R. Jung, M. Metzger, D. Haering, S. Solchenbach, C. Marino, N. Tsiouvaras, C. Stinner, H. A. Gasteiger, *J. Electrochem. Soc.* **2016**, *163*, A1705.
[23] X. Wang, H. Naito, Y. Sone, G. Segami, S. Kuwajima, *J. Electrochem. Soc.* **2005**, *152*, A1996.
[24] H. J. Yang, Y. Jung, *Int. J. Electrochem. Sci.* **2015**, *10*, 9049.
[25] M. Morita, S. Aoki, Y. Matsuda, *Electrochim. Acta* **1992**, *37*, 119.
[26] U. Wietelmann, R. J Bauer, in *Ullmann's Encyclopedia of Industrial Chemistry*, Vol. *21* (Ed: F. Ullmann), Wiley-VCH, Weinheim, **2012**, p. 339.

[27] W. Weng, V. G. Pol, K. Amine, *Adv. Mater.* **2013**, *25*, 1608.
[28] K. A. See, H.-L. Wu, K. C. Lau, M. Shin, L. Cheng, M. Balasubramanian, K. G. Gallagher, L. A. Curtiss, A. A. Gewirth, *ACS Appl. Mater. Interfaces* **2016**, *8*, 34360.
[29] A. Pei, G. Zheng, F. Shi, Y. Li, Y. Cui, *Nano Lett.* **2017**, *17*, 1132.
[30] N. Azimi, Z. Xue, I. Bloom, M. L. Gordin, D. Wang, T. Daniel, C. Takoudis, Z. Zhang, *ACS Appl. Mater. Interfaces* **2015**, *7*, 9169.
[31] C. Zu, N. Azimi, Z. Zhang, A. Manthiram, *J. Mater. Chem. A* **2015**, *3*, 14864.
[32] L. O. Müller, I. Krossing, *Z. Anorg. Allg. Chem.* **2008**, *634*, 962.
[33] X. Zheng, Z. Zhang, G. Tan, X. Wang, *Inorg. Chem.* **2016**, *55*, 1008.
[34] D. Aurbach, O. Youngman, Y. Gofer, A. Meitav, *Electrochim. Acta* **1990**, *35*, 625.
[35] B. D. Adams, J. Zheng, X. Ren, W. Xu, J.-G. Zhang, *Adv. Energy Mater.* **2018**, *8*, 1702097.
[36] D. Lin, Y. Liu, W. Chen, G. Zhou, K. Liu, B. Dunn, Y. Cui, *Nano Lett.* **2017**, *17*, 19.
[37] J. Zhao, L. Liao, F. Shi, T. Lei, G. Chen, A. Pei, J. Sun, K. Yan, G. Zhou, J. Xie, C. Liu, Y. Li, Z. Liang, Z. Bao, Y. Cui, *J. Am. Chem. Soc.* **2017**, *139*, 47.
[38] A. Penas, E. Calvo, M. Pintos, A. Amigo, R. N. Bravo, *J. Chem. Eng. Data* **2000**, *45*, 682.
[39] M. R. Lukatskaya, J. I. Feldblyum, D. G. Mackanic, F. Lissel, D. L. Michels, Y. Cui, Z. Bao, *Energy Environ. Sci.* **2018**, *11*, 2876.
[40] B. Qiao, G. M. Leverick, W. Zhao, A. H. Flood, J. A. Johnson, Y. Shao-Horn, *J. Am. Chem. Soc.* **2018**, *140*, 10932.
[41] K. S. Han, J. Chen, R. Cao, N. N. Rajput, V. Murugesan, L. Shi, H. Pan, J.-G. Zhang, J. Liu, K. A. Persson, K. T. Mueller, *Chem. Mater* **2017**, *29*, 39.
[42] M. Callsen, K. Sodeyama, Y. Tateyama, I. Hamada, *J. Phys. Chem. B* **2017**, *121*, 180.
[43] K. Xu, A. VonCresce, U. Lee, *Langmuir* **2010**, *26*, 11538.
[44] T. Abe, F. Sagane, M. Ohtsuka, Y. Iriyama, Z. Ogumi, *J. Electrochem. Soc.* **2005**, *152*, A2151.
[45] C.-W. Lee, Q. Pang, S. Ha, L. Cheng, S.-D. Han, K. R. Zavadil, K. G. Gallagher, L. F. Nazar, M. Balasubramanian, *ACS Cent. Sci.* **2017**, *3*, 605.
[46] H. Gunther, in *Encyclopedia of Magnetic Resonance* (Eds: R. K. Harris, R. L. Wasylishen), John Wiley & Sons, Ltd., New York **2007**.
[47] I. Swan, M. Reid, P. W. A. Howe, M. A. Connell, M. Nilsson, M. A. Moore, G. A. Morris, *J. Magn. Reson.* **2015**, *252*, 120.
[48] K. Hayamizu, *J. Chem. Eng. Data* **2012**, *57*, 2012.
[49] M. J. Abraham, T. Murtola, R. Schulz, S. Páll, J. C. Smith, B. Hess, E. Lindahl, *SoftwareX* **2015**, *1–2*, 19.
[50] W. L. Jorgensen, D. S. Maxwell, J. Tirado-Rives, *J. Am. Chem. Soc.* **1996**, *118*, 11225.
[51] C. H. Bennett, *J. Comput. Phys.* **1976**, *22*, 245.